LAWRENCE
LIVERMORE
NATIONAL
LABORATORY

LLNL-JRNL-420920

Tungsten spectroscopy relevant to the diagnostics development of ITER divertor plasmas

J. Clementson, P. Beiersdorfer, E. W. Magee, H. S. McLean, R. D. Wood

December 2, 2009

Journal of Physics B: Atomic, Molecular and Optical Physics

Disclaimer

Tungsten spectroscopy relevant to the diagnostics development of ITER divertor plasmas

J. Clementson*, P. Beiersdorfer, E. W. Magee, H. S. McLean, and R. D. Wood

Lawrence Livermore National Laboratory, Livermore, California 94550, USA

Manuscript version 1 December 2009

Abstract. The ITER tokamak will have tungsten divertor tiles and, consequently, the divertor plasmas are expected to contain tungsten ions. The spectral emission from these ions can serve to diagnose the divertor for plasma parameters such as tungsten concentrations, densities, ion and electron temperatures, and flow velocities. The ITER divertor plasmas will likely have densities around 10^{14-15} cm^{-3} and temperatures below 150 eV. These conditions are similar to the plasmas at the Sustained Spheromak Physics Experiment (SSPX) in Livermore. To simulate ITER divertor plasmas, a tungsten impurity was introduced into the SSPX spheromak by prefilling it with tungsten hexacarbonyl prior to the usual hydrogen gas injection and initiation of the plasma discharge. The possibility of using the emission from low charge state tungsten ions to diagnose tokamak divertor plasmas has been investigated using a high-resolution extreme ultraviolet spectrometer.

1. Introduction

The divertor of the ITER tokamak will have tungsten target plates. Tungsten ions will sputter off the surfaces of the tiles at the particle strike points and get introduced into the plasmas. The divertor plasmas will be relatively cool and have large gradients. According to simulations by the ITER Physics Expert Group on Divertor [1], the electron temperatures will mainly be between 25 and 100 eV with peak temperatures around 150 eV close to the X point. Considering the ionization energies of tungsten, see Ref. [2] and Table 1, and neglecting transport, a large fraction of the divertor plasmas can therefore be expected to contain tungsten ions in charge states mainly from three to ten times ionized.

The spectroscopic diagnostics considered for the ITER divertor include optical spectrometers and vacuum ultraviolet (VUV) spectrometers with wavelength coverage down in the soft x-ray region to 10 Å [3, 4]. As demonstrated in this paper, the 150 - 450 Å EUV range seems to offer the best spectral region for monitoring of tungsten in the main divertor volume as the strong resonance lines of several tungsten ions fall in this region. Another advantage of this interval is that expected low-Z impurities, such as

* Also at Department of Physics, Lund University, SE-221 00 Lund, Sweden

carbon ions, offer strong *in situ* wavelength calibration lines, which, in addition, also can serve to measure carbon concentrations. The abundances of tungsten ions in the divertor are of importance for ITER operations as too large quantities entering the confined core plasmas could affect the radiation stability. EUV tungsten spectra would be suitable to infer the concentrations and flow velocities and could, given enough resolution, also be used to measure ion temperatures in the divertor.

To assess where the strong line emission from low charge states of tungsten occur, the structure and spectra of W^{3+} - W^{10+} have been calculated using the Flexible Atomic Code [5]. The spectra have been modeled under magnetic fusion plasma conditions in the 100 - 1100 Å spectral range. Synthetic spectra of W^{5+} - W^{16+} in the 100 - 500 Å region have previously been presented by Peacock *et al.* in their review of anticipated x-ray and VUV radiation in ITER [6].

Previously, the spectra of neutral to six-times ionized tungsten have been studied [7, 8]. However, little focus has been given to the EUV range (150 - 450 Å) where, for charge states above four-times ionized, strong resonance transitions are expected. The VUV spectrum of trebly ionized Lu-like W IV has been studied down to 673 Å by Iglesias *et al.* [9] using a sliding-spark discharge. The spectrum of quadruply ionized tungsten, W V, isoelectronic to ytterbium, was first studied by Meijer using a sliding spark, leading to the identification of lines down to 638 Å [10]. Later studies by Kildiyarova *et al.* [11] and Churilov *et al.* [12], also using spark sources, observed lines down to 417 and 391 Å, respectively. The sixth spectrum of tungsten, Tm-like W VI, was also first investigated by Meijer [13] and later by Kaufman and Sugar [14, 15] resulting in wavelength measurements down to 382 Å. Sugar and Kaufman also observed Er-like W VII, again using a sliding spark, and their measurement yielded wavelengths down to 130 Å [16]. Wyart *et al.* re-examined those spectra and identified a number of lines in the 316 - 345 Å range [17]. A low-resolution observation of Ho-like W VIII in a tokamak plasma by Veres *et al.*, indicated emission around 190 and 235 Å [18]. The spectra of higher charge states have, to our knowledge, not been investigated in any wavelength band until the tentative identification of thirteen-times ionized Pm-like W XIV, which Hutton *et al.* may have observed at the Berlin electron beam ion trap [19, 20, 21]. With the exception of Er-like W VII, low-charge tungsten spectra have not been studied in the EUV.

To simulate tungsten emission from ITER divertor plasmas, hydrogen discharges with trace amounts of tungsten have been produced at the Sustained Spheromak Physics Experiment facility (SSPX) at the Lawrence Livermore National Laboratory [22, 23, 24]. The SSPX spheromak, which was decommissioned in 2007, had plasma conditions comparable to those expected in the ITER divertor, with typical electron temperatures of around 100 eV and densities in the 10^{14-15} cm^{-3} range. The tungsten emission from SSPX plasmas can hence be assumed similar to those of the future ITER divertor or other magnetic fusion experiments operating in this low-temperature, high-density regime. The SSPX plasmas contained trace amounts of tungsten resulting from the usage of tungsten as a plasma-facing material coating the flux conserver. In addition

to this intrinsic tungsten, a novel sublimation injector was constructed to increase the concentration of tungsten impurity ions in the spheromak plasmas. These tungsten-doped plasmas were studied spectroscopically using a 5.6 m grazing-incidence EUV spectrometer.

2. Spectral Modeling

Based on ionization energies, the tungsten ions that can be expected to dominate the charge balance in the main plasma volume of the ITER divertor are Lu-like W^{3+} up to around Gd-like W^{10+}, see Table 1. The spectra of these tungsten charge states have been calculated to guide the spheromak measurement and assess in which wavelength range the strong transitions occur. Even though some of these spectra have been studied experimentally in the past, those studies have been done at densities different than those found in magnetic fusion plasmas and, hence, line intensities can be quite different.

The calculations were performed using the Flexible Atomic Code, FAC v1.1.1., written by Gu [5]. The structure of the ions was calculated with closed K, L, and M shells. Depending on spectral complexity, different numbers of energy levels and configuration interactions were included. Considered transitions comprise those involving ground configurations with valence electrons in $n = 5$, and excited configurations with one electron excited from the 4f subshell to $n = 5$ or 6, and electrons excited within the $n = 5$ shell or from $n = 5$ - n' = 6. These multi-electron spectra are quite difficult to calculate with any accuracy because configuration interaction effects are large, as noted by Sugar and Kaufman for Er-like W VII [16]. Comparisons with known line positions of W VII indicate that the calculated wavelengths are within 20 Å of the measured values. To aid the spectral analysis of the SSPX data, the low-Z impurity species were also calculated, i.e. carbon, nitrogen, and oxygen. These systems were modeled with levels up to $n = 5$. Here, comparisons with known line positions listed by Kelly [25] show that most calculated line positions are within 10 Å of the experimental wavelengths.

The spectra were modeled at various electron temperatures and densities in order to have reference spectra from which to infer the SSPX temperatures. Spectra were calculated at densities of 10^{14} and 10^{15} cm^{-3}, but very little difference on the emission signatures was seen. However, as expected, the temperature had a strong effect and the spectra were therefore calculated in the 25 - 200 eV interval. The collisional-radiative spectral models include collisional excitation and de-excitation and autoionization. An overview of the tungsten spectra is shown in Fig. 1 for $T_e = 100$ eV. It is clear that for charge states above four-times ionized, Yb-like W V, the strong line radiation falls in the EUV region. It is also worth noting that the emissivities drop to very low values for ions above Ho-like W VIII, which means that for ITER divertor plasmas it is likely that only the very low charge states will be of interest for spectroscopic diagnostics. The spectra of Tm-like W VI, Er-like W VII, and Ho-like W VIII are presented in greater detail in Fig. 2, where they are modeled in the 150 - 450 Å range at various temperatures with

a resolution of $\Delta\lambda = 0.3$ Å full width at half maximum (fwhm). The low-Z reference spectra at $T_e = 50$ eV are also presented, see Figs. 3, 4, and 5. All spectra are calculated at $n_e = 10^{14}$ cm^{-3}.

3. Experimental setup

The tungsten study was performed at the SSPX spheromak facility, a small-size fusion experiment in Livermore [22, 23, 24]. The SSPX device produced self-organized toroidal plasmas lasting a few milliseconds. The tungsten was injected into the magnetically confined plasmas in the form of tungsten hexacarbonyl, $W(CO)_6$, a crystalline compound that also has been introduced into the Livermore SuperEBIT electron beam ion trap for spectroscopic investigations of highly charged tungsten ions [26, 27]. Here, 5 grams of tungsten hexacarbonyl was placed in a 1-liter volume, which had been cleaned and purged with nitrogen gas. The volume was then evacuated to approximately 10^{-5} Torr and heated using wrapped heater tapes. The pressure increase was monitored with a vacuum gauge and pressures were varied from 0.1 to 2 Torr by changing the temperature, which was recorded with a thermocouple. The tungsten hexacarbonyl volume, which was connected to a view port of SSPX, was opened during the hydrogen prefill phase approximately 0.5 s prior to the discharge. As the tungsten gas pressures were higher than the SSPX vacuum vessel pressure, the gas could easily stream through a solenoid-controlled valve into the spheromak.

A high-resolution grazing-incidence spectrometer was used to study the tungsten emission. The instrument has previously been used to study titanium and low-Z plasma impurities on SSPX [28, 29, 30, 31] and is described in detail in Ref. [32]. For this experiment the spectrometer was equipped with a Photometrics back-illuminated charge-coupled device (CCD) detector and a 30 μm entrance slit. With a field of view tangential to the magnetic axis of the spheromak the observed emission originated both from the cooler edge and the hottest part at the center of the plasma.

The spheromak plasmas were studied with and without tungsten injection to support the line identification process. The toroidal plasma current was used to change the electron temperature. Record peak temperatures at SSPX have been noted to exceed 500 eV [23], however for this experiment the temperatures were likely in the 25 - 100 eV range. As the Thomson scattering electron-temperature diagnostic was offline, the plasma temperatures had to be inferred from the calculated spectra. The injection of tungsten into SSPX did not seem to have any negative effect on the spheromak performance and plasma currents of up to around 1 MA were achieved during the few-millisecond discharges.

4. Analysis and Results

Figures 6, 7, and 8 show SSPX spectra in three regions where tungsten lines appear. The spectra were *in situ* wavelength calibrated using L-shell lines from carbon and oxygen.

These lines, which also got enhanced during injection of tungsten hexacarbonyl, were observed in first and second order. In addition to this emission, spectra were also observed from nitrogen, titanium, and copper. The spectral lines were identified using the calculated spectra for line intensities and line lists from Kelly [25] for line positions. Even though the calculated wavelengths sometimes were slightly off, the intensities generally agreed pretty well with the observed spectra. Lines that did not match any known spectra were likely candidates for being tungsten lines. Additionally, tungsten line identification was helped by the fact that the amounts of injected tungsten changed the spectra and that the predicted emission of a number of potential tungsten lines were observed. Identified tungsten lines are listed in Table 2, and unclassified candidate lines are listed in Table 3.

The tungsten emission is dominated by Er-like W VII, which shows in most spectra. The Er-like lines are identified based on the classifications by Sugar and Kaufman [16]. However, the line intensities given by Sugar and Kaufman do not agree with the observed SSPX intensities, which is likely due to the different densities of the emitting plasmas. The 216 Å line is generally the strongest line followed by the 261 Å line. The 289 Å line overlaps with a carbon line prohibiting a clear determination of its intensity, which according to the modeling should be very low. The 294 Å line is weaker and the 302 Å line much stronger than the calculations suggest. It is possible that the stronger intensity of the 302 Å line is due to a line blend. However, as noted earlier, these spectra are difficult to predict and even though Er-like W VII, with its closed shell structure, should be the easiest to calculate, it is quite possible that the calculated spectra are not that accurate. The line at 313 Å is slightly off the value given by Sugar and Kaufman [16], which could mean that it is blended, too. Some of the lines identified by Wyart *et al.* [17] possibly show around 330 - 340 Å as weak features.

Based on the calculations, two groups of lines are believed to originate mainly from Ho-like W VIII. Ho-like W has previously been observed in a tokamak plasma at around 190 and 235 Å by Veres *et al.* [18]. However, the features in the SSPX spectra are shifted towards longer wavelengths relative the tokamak spectrum at around 202 and 255 Å. No reference lines were shown or discussed in Ref. [18], and a possible explanation of the shift could therefore be that the tokamak spectrometer had not been sufficiently calibrated.

Two 5d - 5f transitions from Tm-like W VI are observed at 382 and 394 Å. Those are the shortest wavelengths previously measured in Tm-like W [14, 15]. The FAC calculations give several isolated Tm-like W lines in the EUV region, especially in the 200 - 240 Å range. These are not easy to identify, because there are plenty of lines in this region, including the Ho-like W candidate lines, and the calculations are not accurate enough to identify individual lines. The calculated lines can be both longer as well as shorter than the true line positions, and therefore the relative positions of the calculated lines may change. The Tm-like candidate lines could be blended or interchanged with the Ho-like W candidate lines. Since many of the tungsten ions have several transitions around 200 Å, it is also possible that contributions from other charge states are blending

with the candidate lines, in addition to the intrinsic impurity ions.

Several tungsten candidate lines have been identified. These lines are designated with red labels in the spectra. Based on the calculations transitions are listed in Table 3 with suggested line positions. Considering the agreement with the Er-like W lines, it is likely that the calculated wavelengths are within 20 Å of actual values.

5. Summary

The tungsten emission from the SSPX plasmas is dominated by Er-like W VII with contributions from Tm-like W VI and Ho-like W VIII. The prevalence of Er-like W is likely due to the closed $4f^{14}5s^25p^6$ ground configuration, making the ion abundant over a large temperature interval. In addition to this, Er-like W has strong isolated lines, which makes it very suitable for plasma diagnostics, especially to infer tungsten concentrations, ion temperatures, and flow velocities.

However, even though the SSPX plasmas only show three charge states, it is quite possible that transport can affect the charge balance to look somewhat different in the ITER divertor. As indicated by the FAC calculations, the 150 - 450 Å spectral band contains strong emission from several charge states. Accurate atomic data on these ions are necessary in order to realize tungsten spectroscopy as a viable divertor diagnostic. Although tungsten line positions can be determined from tungsten-doped plasmas, unambiguous line identifications can prove difficult as lines from neighboring charge states often seem to be close and may even overlap. In order to disentangle the emission and analyze relative line intensities, we are planning to extend this investigation at the Livermore low-energy electron beam ion trap.

Acknowledgments

This work was performed under the auspices of the United States Department of Energy by Lawrence Livermore National Laboratory under contract DE-AC52-07NA-27344. The authors would like to acknowledge technical, experimental, and theoretical support from Bob Geer, Rick Kemptner, Steven Gordon, Josh King, Dr. Ming Feng Gu, and the SSPX group. Joel Clementson would like to thank Dr. Hans Lundberg, Dr. Sven Huldt, and Prof. Sune Svanberg for their support.

References

[1] ITER Physics Expert Group on Divertor 1999 *Nucl. Fusion* **39** 2391–2469
[2] Kramida A E and Reader J 2006 *At. Data Nucl. Data Tables* **92** 457–479
[3] Sugie T, Costley A, Malaquias A and Walker C 2003 *J. Plasma Fusion Res.* **79** 1051–1061
[4] Skinner C H 2008 *Can. J. Phys.* **86** 285–290
[5] Gu M F 2008 *Can. J. Phys.* **86** 675–689
[6] Peacock N J, O'Mullane M G, Barnsley R and Tarbutt M 2008 *Can. J. Phys.* **86** 277–284
[7] Kramida A E and Shirai T 2006 *J. Phys. Chem. Ref. Data* **35** 423–683
[8] Kramida A E and Shirai T 2009 *At. Data Nucl. Data Tables* **95** 305–474

[9] Iglesias L, Kaufman V, Garcia-Riquelme O and Rico F R 1985 *Phys. Scr.* **31** 173–183
[10] Meijer F G 1986 *Physica* **141C** 230–236
[11] Kildiyarova R R, Churilov S S and Joshi Y N 1996 *Phys. Scr.* **53** 454–460
[12] Churilov S S, Kildiyarova R R and Joshi Y N 1996 *Can. J. Phys.* **74** 145–149
[13] Meijer F G 1974 *Physica* **73** 415–420
[14] Kaufman V and Sugar J 1976 *J. Opt. Soc. Am.* **66** 1019–1025
[15] Sugar J and Kaufman V 1979 *J. Opt. Soc. Am.* **69** 141–143
[16] Sugar J and Kaufman V 1975 *Phys. Rev. A* **12** 994–1012
[17] Wyart J F, Kaufman V and Sugar J 1981 *Phys. Scr.* **23** 1069–1078
[18] Veres G, Bakos J S and Kardon B 1996 *J. Quant. Spectrosc. Radiat. Transfer* **56** 295–301
[19] Hutton R, Zou Y, Reyna Almandos J, Biedermann C, Radtke R, Greier A and Neu R 2003 *Nucl. Instr. and Meth. in Phys. Res. B* **205** 114–118
[20] Wu S and Hutton R 2008 *Can. J. Phys.* **86** 125–129
[21] Träbert E, Vilkas M J and Ishikawa Y 2009 *J. Phys. Conf. Ser.* **163** 012017
[22] Hooper E B, Pearlstein L D and Bulmer R H 1999 *Nucl. Fusion* **39** 863–871
[23] Hudson B, Wood R D, McLean H S, Hooper E B, Hill D N, Jayakumar J, Moller J, Montez D, Romero-Talamás C A, Casper T A, Johnson III J A, LoDestro L L, Mezonlin E and Pearlstein L D 2008 *Phys. Plasmas* **15** 056112
[24] Wood R D, Hill D N, Hooper E B, Woodruff S, McLean H S and Stallard B W 2005 *Nucl. Fusion* **45** 1582–1588
[25] Kelly R L 1987 *J. Phys. Chem. Ref. Data* **16** Suppl. 1
[26] Clementson J, Beiersdorfer P, Brown G V and Gu M F 2009 *Phys. Scr.* Accepted
[27] Clementson J, Beiersdorfer P and Gu M F 2009 *Phys. Rev. A* Submitted
[28] Graf A T, Brockington S, Horton R, Howard S, Hwang D, Beiersdorfer P, Clementson J, Hill D, May M, Mclean H, Wood R, Bitter M, Terry J, Rowan W L, Lepson J K and Delgado-Aparicio L 2008 *Can. J. Phys.* **86** 307–313
[29] Clementson J, Beiersdorfer P, Gu M F, McLean H S and Wood R D 2008 *J. Phys. Conf. Ser.* **130** 012004
[30] Clementson J H T, Beiersdorfer P and Wood R D 2009 *J. Phys. Conf. Ser.* **163** 012018
[31] Wilcox P G, Safronova A S, Kantsyrev V L, Safronova U I, Williamson K M, Yilmaz M F, Clementson J, Beiersdorfer P and Struve K W 2008 *Rev. Sci. Instrum.* **79** 10F543
[32] Clementson J, Beiersdorfer P and Magee E W 2008 *Rev. Sci. Instrum.* **79** 10F538

Table 1. Tungsten ionization energies (IE) excerpt from Kramida and Reader [2].

Ion	IE (eV)	Ion	IE (eV)
Neutral W	7.864	Ho-like W^{7+}	141.2
Ta-like W^{+}	16.37	Dy-like W^{8+}	160.2
Hf-like W^{2+}	26.0	Tb-like W^{9+}	179.0
Lu-like W^{3+}	38.2	Gd-like W^{10+}	208.9
Yb-like W^{4+}	51.6	Eu-like W^{11+}	231.6
Tm-like W^{5+}	64.77	Sm-like W^{12+}	258.2
Er-like W^{6+}	122.01	Pm-like W^{13+}	290.7

Table 2. Observed tungsten lines in the SSPX spheromak. [a]Sugar and Kaufman [16], [b]Kaufman and Sugar [14, 15]

Ion	Experiment λ (Å)	Prev. Exp. λ (Å)	Theory λ (Å)	Transition lower level	upper level
Er	188.15	188.159[a]	193.4	$(4f^{14}5s^25p^6)_0$	$(4f^{14}5s^25p_{1/2}5p^4_{3/2}6s_{1/2})_1$
Er	216.19	216.219[a]	203.2	$(4f^{14}5s^25p^6)_0$	$(4f^{14}5s^25p_{1/2}5p^4_{3/2}5d_{3/2})_1$
Er	223.82	223.846[a]	233.2	$(4f^{14}5s^25p^6)_0$	$(4f^{14}5s^25p^2_{1/2}5p^3_{3/2}6s_{1/2})_1$
Er	261.35	261.387[a]	254.9	$(4f^{14}5s^25p^6)_0$	$(4f^{14}5s^25p^2_{1/2}5p^3_{3/2}5d_{5/2})_1$
Er	289.44	289.526[a]	301.2	$(4f^{14}5s^25p^6)_0$	$(4f^5_{5/2}4f^8_{7/2}5s^25p^65d_{5/2})_1$
Er	294.37	294.376[a]	290.9	$(4f^{14}5s^25p^6)_0$	$(4f^5_{5/2}4f^8_{7/2}5s^25p^65d_{3/2})_1$
Er	302.28	302.272[a]	320.0	$(4f^{14}5s^25p^6)_0$	$(4f^6_{5/2}4f^7_{7/2}5s^25p^65d_{5/2})_1$
Er	313.64	313.573[a]	303.9	$(4f^{14}5s^25p^6)_0$	$(4f^{14}5s^25p^2_{1/2}5p^3_{3/2}5d_{3/2})_1$
Tm	382.12	382.145[b]	371.9	$(4f^{14}5s^25p^65d_{3/2})_{3/2}$	$(4f^{14}5s^25p^65f_{5/2})_{5/2}$
Tm	394.08	394.133[b]	382.7	$(4f^{14}5s^25p^65d_{5/2})_{5/2}$	$(4f^{14}5s^25p^65f_{7/2})_{7/2}$

Table 3. Candidate tungsten transitions in the SSPX spheromak.

Ion	Transition lower level	upper level	Theory λ (Å)	Exp. candidate lines λ (Å)
Ho	$(4f^{14}5s^25p^2_{1/2}5p^3_{3/2})_{3/2}$	$(4f^{14}5s^25p_{1/2}5p^3_{3/2}5d_{3/2})_{3/2}$	193.2	194.5, 198.0, 198.8
Ho	$(4f^{14}5s^25p^2_{1/2}5p^3_{3/2})_{3/2}$	$(4f^{14}5s^25p_{1/2}5p^3_{3/2}5d_{3/2})_{1/2}$	195.9	198.0, 198.8, 200.5
Ho	$(4f^{14}5s^25p^2_{1/2}5p^3_{3/2})_{3/2}$	$(4f^{14}5s^25p_{1/2}5p^3_{3/2}5d_{3/2})_{5/2}$	197.5	201.8
Ho	$(4f^{14}5s^25p_{1/2}5p^4_{3/2})_{1/2}$	$(4f^{14}5s^25p^4_{3/2}5d_{3/2})_{3/2}$	199.0	198.0, 198.8, 200.5, 205.3
Ho	$(4f^{14}5s^25p^2_{1/2}5p^3_{3/2})_{3/2}$	$(4f^{14}5s^25p_{1/2}5p^3_{3/2}5d_{3/2})_{3/2}$	202.3	200.5, 205.3, 208.0
Tm	$(4f^{14}5s^25p^65d_{3/2})_{3/2}$	$(4f^{14}5s^25p_{1/2}5p^4_{3/2}5d^2_{3/2})_{3/2}$	202.5	198.0, 198.8, 200.5, 201.8, 205.3, 208.0
Tm	$(4f^{14}5s^25p^65d_{5/2})_{5/2}$	$(4f^{14}5s^25p_{1/2}5p^4_{3/2}5d_{3/2}5d_{5/2})_{5/2}$	206.7	205.3, 208.0, 211.0
Tm	$(4f^{14}5s^25p^65d_{5/2})_{5/2}$	$(4f^{14}5s^25p_{1/2}5p^4_{3/2}5d_{3/2}5d_{5/2})_{3/2}$	206.9	205.3, 208.0, 210.2, 211.0
Tm	$(4f^{14}5s^25p^65d_{5/2})_{5/2}$	$(4f^{14}5s^25p_{1/2}5p^4_{3/2}5d_{3/2}5d_{5/2})_{7/2}$	212.2	205.3, 208.0, 210.2, 211.0
Ho	$(4f^{14}5s^25p_{1/2}5p^4_{3/2})_{1/2}$	$(4f^{14}5s^25p_{1/2}5p^3_{3/2}5d_{5/2})_{1/2}$	222.0	211.0, 218.4, 229.8
Tm	$(4f^{14}5s^25p^65d_{3/2})_{3/2}$	$(4f^{14}5s^25p_{1/2}5p^4_{3/2}5d^2_{3/2})_{5/2}$	228.4	218.4, 229.8, 240.0, 241.8
Ho	$(4f^{14}5s^25p^2_{1/2}5p^3_{3/2})_{3/2}$	$(4f^{14}5s^25p^2_{1/2}5p^2_{3/2}5d_{5/2})_{5/2}$	249.0	253.7, 254.3, 255.4, 259.3
Ho	$(4f^{14}5s^25p^2_{1/2}5p^3_{3/2})_{3/2}$	$(4f^{14}5s^25p^2_{1/2}5p^2_{3/2}5d_{5/2})_{3/2}$	251.8	253.7, 254.3, 255.4, 259.3
Er	$(4f^5_{5/2}4f^8_{7/2}5s^25p^65d_{3/2})_1$	$(4f^5_{5/2}4f^8_{7/2}5s^25p^65f_{5/2})_0$	260.6	259.3, 276.2
Ho	$(4f^{14}5s^25p^2_{1/2}5p^3_{3/2})_{3/2}$	$(4f^5_{5/2}4f^8_{7/2}5s^25p^2_{1/2}5p^3_{3/2}5d_{3/2})_{3/2}$	261.0	253.7, 254.3, 255.4, 259.3, 276.2
Ho	$(4f^{14}5s^25p^2_{1/2}5p^3_{3/2})_{3/2}$	$(4f^6_{5/2}4f^7_{7/2}5s^25p^2_{1/2}5p^3_{3/2}5d_{5/2})_{5/2}$	263.1	253.7, 254.3, 255.4, 259.3, 276.2
Er	$(4f^{14}5s^25p^2_{1/2}5p^3_{3/2}5d_{5/2})_1$	$(4f^{14}5s^25p^2_{1/2}5p^3_{3/2}5f_{7/2})_2$	370.1	376.3

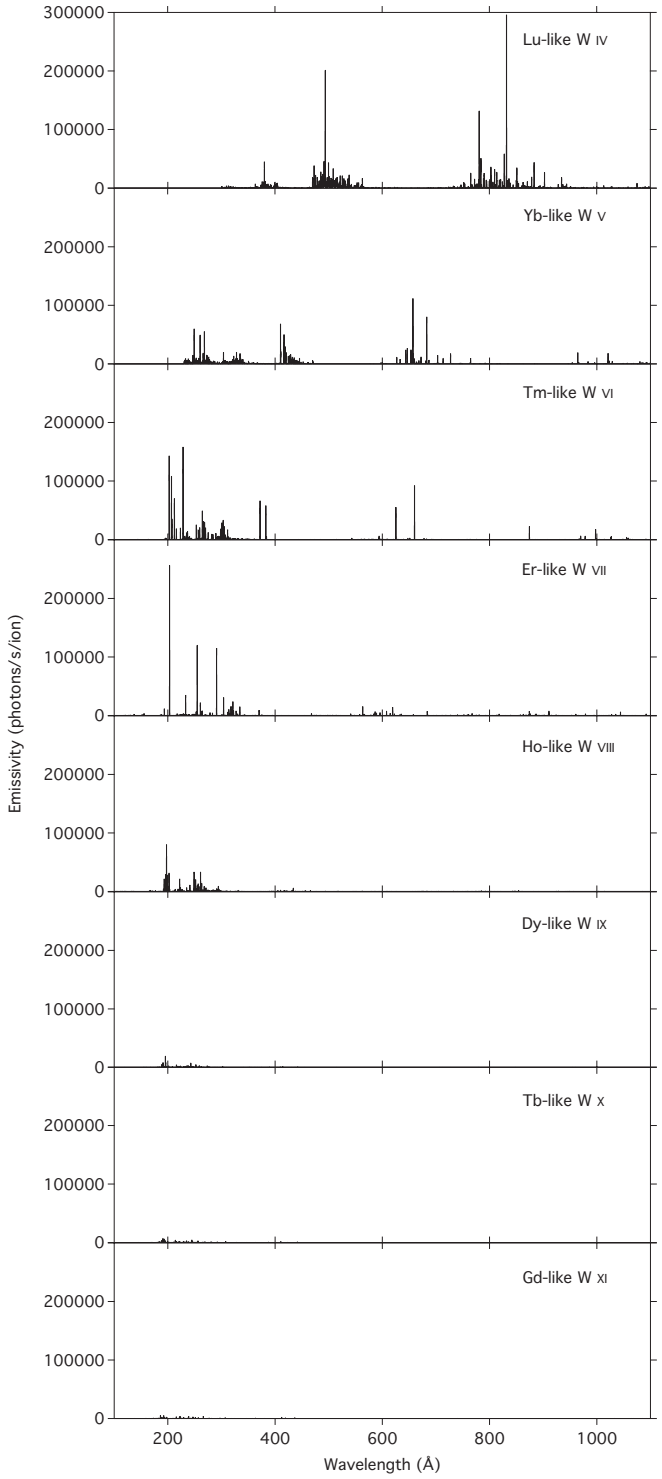

Figure 1. Calculated tungsten spectra at $T_e = 100$ eV and $n_e = 10^{14}$ cm^{-3}. The emissivity scale has break set to the same value for each charge state in order to provide a direct comparison of the expected line intensities.

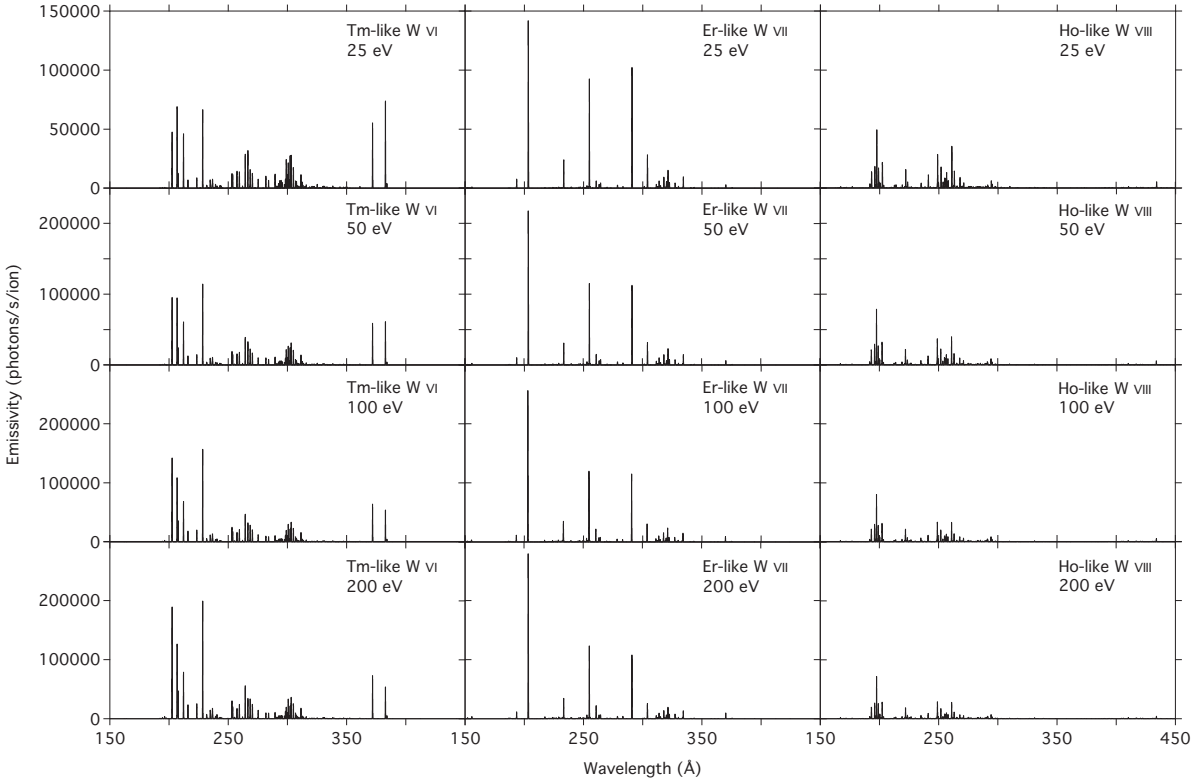

Figure 2. Calculated tungsten spectra at $n_e = 10^{14}$ cm^{-3} with $\Delta\lambda = 0.3$ Å fwhm. The spectra are labeled according to charge state and electron temperature.

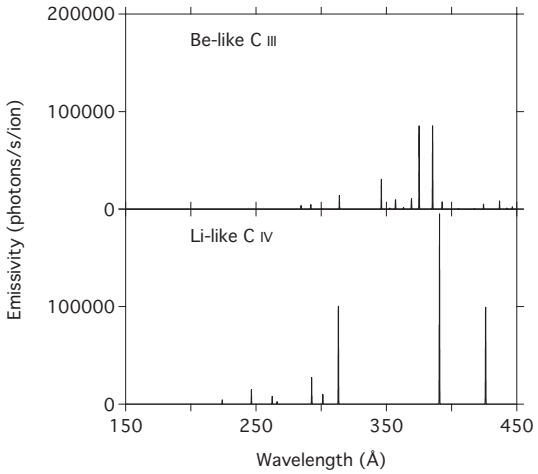

Figure 3. Calculated carbon spectra at $T_e = 50$ eV and $n_e = 10^{14}$ cm^{-3} with $\Delta\lambda = 0.3$ Å fwhm.

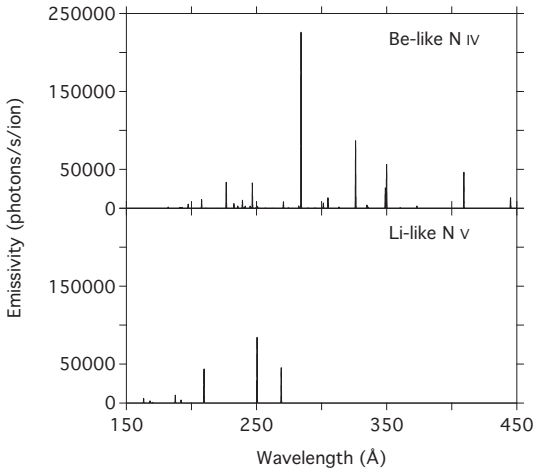

Figure 4. Calculated nitrogen spectra at $T_e = 50$ eV and $n_e = 10^{14}$ cm^{-3} with $\Delta\lambda =$ 0.3 Å fwhm.

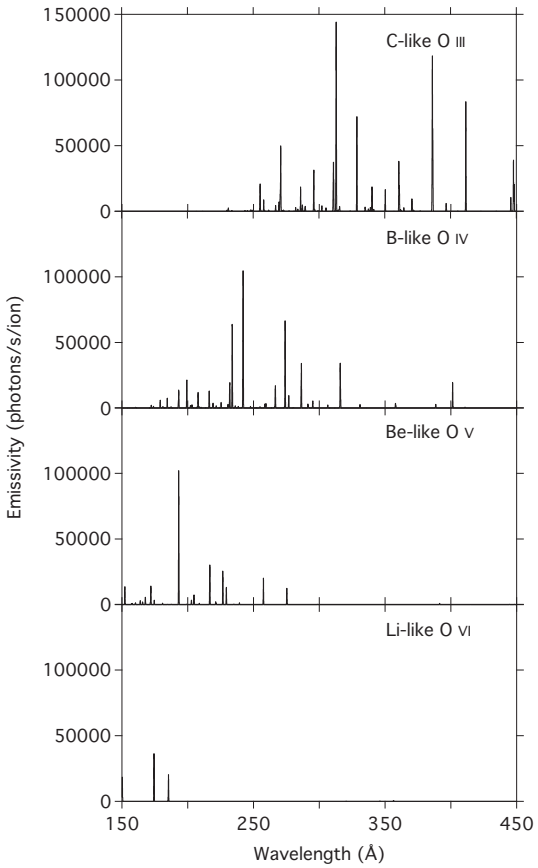

Figure 5. Calculated oxygen spectra at $T_e = 50$ eV and $n_e = 10^{14}$ cm^{-3} with $\Delta\lambda =$ 0.3 Å fwhm.

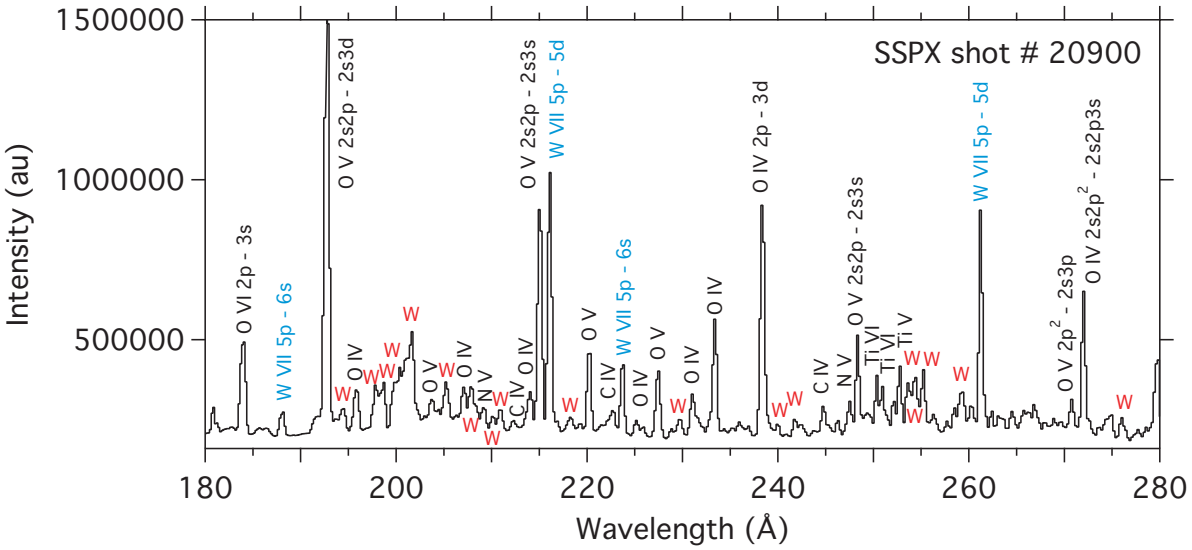

Figure 6. SSPX shot # 20900. Low-temperature spheromak plasma with tungsten hexacarbonyl injection. Tungsten lines are designated with blue labels and tungsten candidate lines with red labels. Also shown are lines from carbon, nitrogen, oxygen, and titanium.

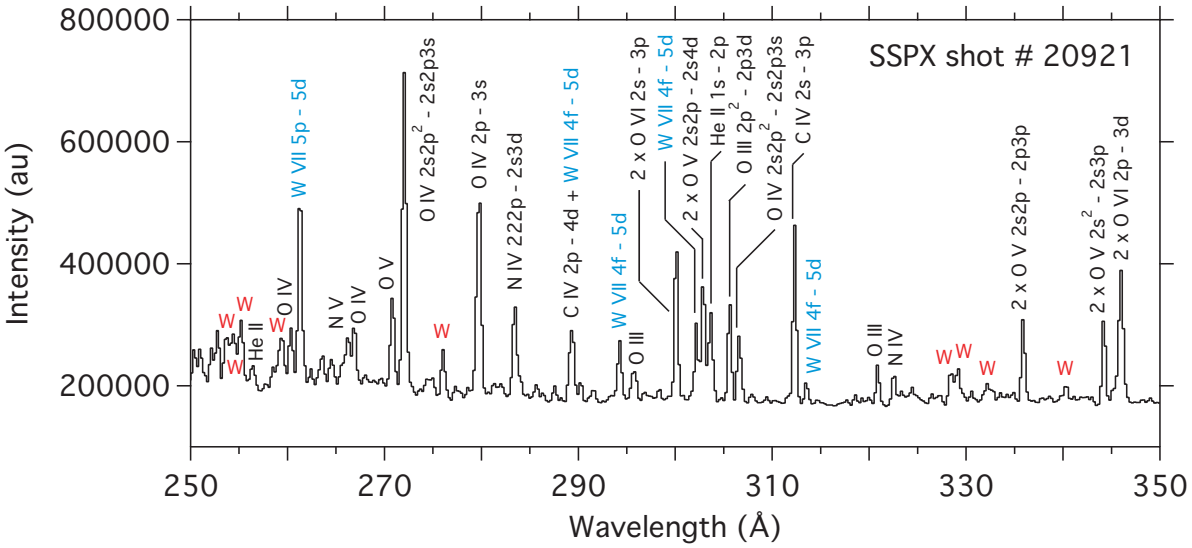

Figure 7. SSPX shot # 20921. Low-temperature spheromak plasma with tungsten hexacarbonyl injection. Tungsten lines are designated with blue labels and tungsten candidate lines with red labels. Also shown are lines from carbon, nitrogen, oxygen, and titanium.

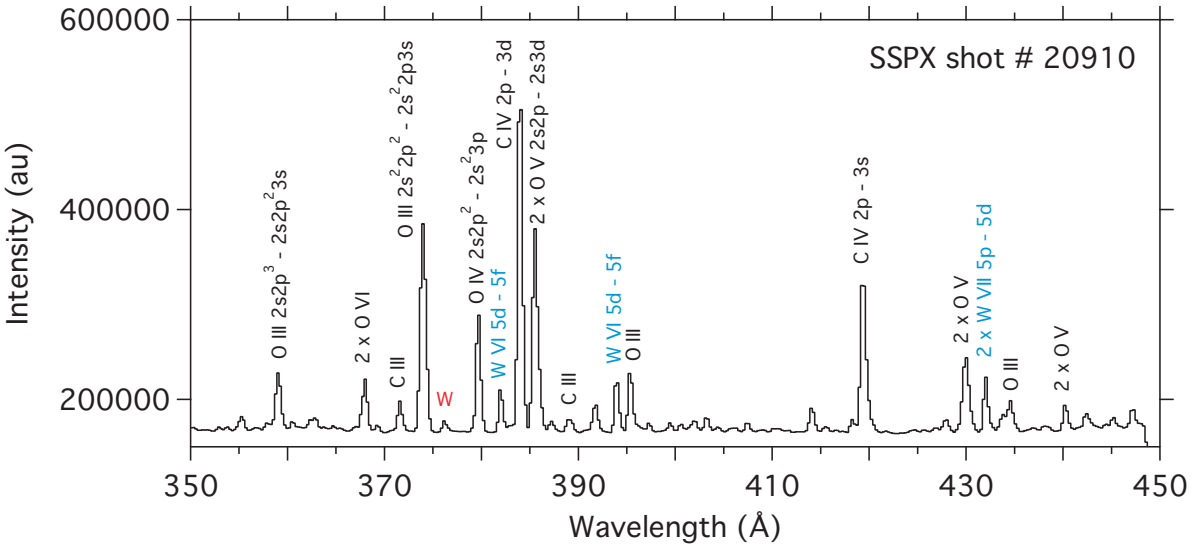

Figure 8. SSPX shot # 20910. Low-temperature spheromak plasma with tungsten hexacarbonyl injection. Tungsten lines are designated with blue labels and tungsten candidate lines with red labels. Also shown are lines from carbon, nitrogen, oxygen, and titanium.